nature structural & molecular biology

Dynamic switch of the signal recognition particle from scanning to targeting

Wolf Holtkamp, Sejeong Lee, Thomas Bornemann, Tamara Senyushkina, Marina V Rodnina & Wolfgang Wintermeyer

Ribosomes synthesizing inner membrane proteins in *Escherichia coli* are targeted to the membrane by the signal recognition particle (SRP) pathway. By rapid kinetic analysis we show that after initial binding to the ribosome, SRP undergoes dynamic fluctuations in search of additional interactions. Non-translating ribosomes, or ribosomes synthesizing non-membrane proteins, do not provide these contacts, allowing SRPs to dissociate rapidly. A nascent peptide in the exit tunnel stabilizes SRPs in a standby state. Binding to the emerging signal-anchor sequence (SAS) of a nascent membrane protein halts the fluctuations of SRP, resulting in complex stabilization and recruitment of the SRP receptor. We propose a kinetic model where SRP rapidly scans all ribosomes until it encounters a ribosome exposing an SAS. Binding to the SAS switches SRP into the targeting mode, in which dissociation is slow and docking of the SRP receptor is accelerated.

Proteins of the inner membrane in *E. coli* are inserted into the membrane in a co-translational manner. Ribosomes that synthesize membrane proteins are targeted to the protein-conducting channel (translocon) in the membrane via the SRP pathway[1–3]. The signal for a translating ribosome to enter the SRP pathway and dock to the translocon is the appearance of a hydrophobic signal sequence of about 20 amino acids that is recognized by SRP, the SAS. The signal sequence is often located near the N terminus and forms the first transmembrane helix of the membrane protein. Translating ribosomes exposing an SAS bind SRP with high affinity (K_d < 1 nM)[4,5]. The ribosome-bound SRP recruits the SRP receptor, FtsY in bacteria, in a GTP-dependent manner[4]. A high-affinity complex of translating ribosomes, SRP, and FtsY is also formed when the peptide exit tunnel is filled with a nascent peptide of a length of 30–35 amino acids, independent of its sequence, and no SAS is exposed outside the ribosome[4]. Ribosome–nascent chain complexes (RNCs) subsequently exposing an SAS are transferred from the targeting complex to the translocon for co-translational membrane insertion. By contrast, the appearance of a non-SAS peptide outside the exit tunnel weakens SRP binding[4], resulting in the rejection of the respective RNC from the targeting complex and the continuation of translation in the cytosol.

The affinity of SRP binding to non-translating ribosomes, although it is about two orders of magnitude lower than the affinity of binding to RNCs exposing an SAS, nevertheless is still rather high (≈0.1 μM)[4]. In addition, SRP can bind to RNCs exposing non-SAS sequences as well—that is, to RNCs that are not designated for targeting—albeit with low affinity[4,5]. As the concentration of ribosomes in the cell is high (10 μM or higher, depending on growth conditions), the affinity difference between ribosomes exposing an SAS and other ribosomes, including non-translating ones, may become insufficient for the discrimination between correct and incorrect RNCs. Furthermore, the concentration of SRP in the cell is low, amounting to only a few percent of the total concentration of ribosomes[6]. Thus, if discrimination were purely thermodynamic, most of the SRP would be sequestered in unproductive complexes, unavailable for timely membrane targeting of ribosomes synthesizing membrane proteins. One possible solution to this conundrum is that the dissociation of unproductive complexes is rapid despite a relatively high binding affinity. Kinetically unstable binding of SRP to non-translating ribosomes or ribosomes synthesizing non-membrane proteins would allow SRP to scan many ribosomes until it recognizes a ribosome exposing an SAS and initiates membrane targeting by recruiting FtsY.

We set out to examine the kinetics of SRP-ribosome interactions, asking how SRP can scan different ribosomes for exposed nascent signal sequences without being trapped in unproductive complexes. We measured the kinetics of complex formation between SRP, FtsY, and ribosomes in various functional states, including non-translating ribosomes and RNCs carrying nascent chains of varying kinds; these nascent chains included one with the N-terminal SAS of leader peptidase as well as one exposing the non-SAS sequence of HemK, a cytosolic protein. To distinguish the contributions of SRP-ribosome and SRP-SAS interactions to the stabilization of the complex, we have also studied the effect of binding an isolated peptide encompassing an SAS to SRP on the ribosome.

RESULTS

Kinetic stability of SRP–ribosome complexes

To probe the kinetics of SRP–ribosome complex formation and dissociation, we monitored FRET between fluorescent labels attached to the ribosome and to SRP. The FRET donor was MDCC at position 21

Department of Physical Biochemistry, Max Planck Institute for Biophysical Chemistry, Göttingen, Germany. Correspondence should be addressed to W.W. (wolfgang.wintermeyer@mpibpc.mpg.de).

Received 24 May; accepted 21 September; published online 11 November 2012; doi:10.1038/nsmb.2421

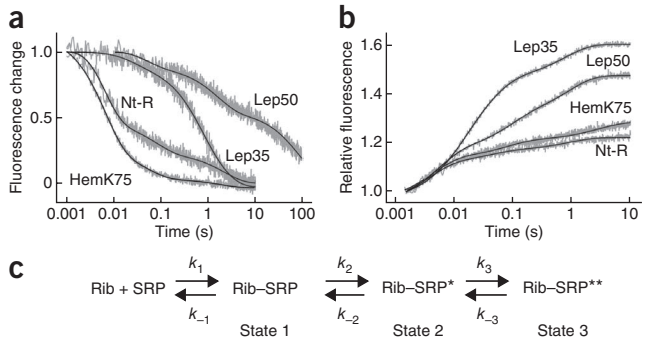

Figure 1 Kinetics of SRP–ribosome interaction. (**a**) Dissociation of SRP from ribosomes or RNCs. Complexes of MDCC-labeled non-translating ribosomes (Nt-R), HemK75-RNCs, Lep35-RNCs or Lep50-RNCs (0.05 μM final concentration after mixing) with Bpy-labeled SRP (0.1 μM) were rapidly mixed with non-labeled SRP (2 μM) in a stopped-flow apparatus. Dissociation was monitored by FRET, measuring Bpy (acceptor) fluorescence. The amplitudes of the fluorescence decreases were comparable and are plotted in normalized form. Continuous lines represent the functions obtained by global fitting of all time courses of complex formation (**Supplementary Fig. 2**) and dissociation on the basis of a three-step model (compare with **c**). (**b**) SRP complex formation with non-translating ribosomes and RNCs. MDCC-labeled vacant ribosomes (Nt-R) or RNCs (25 nM final concentration after mixing) were rapidly mixed with Bpy-labeled SRP (0.75 μM). Complex formation was monitored by the increase of Bpy fluorescence due to FRET. (**c**) Three-step scheme of SRP–ribosome (Rib) complex formation. Global fitting of the time courses for binding and dissociation measured at different concentrations (see Online Methods) yielded the values of the rate constants summarized in **Table 1**.

in ribosomal protein L23, which is located at the peptide exit of the ribosome and forms part of the SRP binding site[7]. The acceptor was Bodipy FL (Bpy) at position 430 in the M domain of Ffh. We expected high FRET efficiency for the complex, as the donor-acceptor separation of 20 Å, estimated from structural models of SRP complexes with translating ribosomes[8,9], is well below the critical distance of 50% FRET efficiency for the two fluorophores (R_o = 50 Å). RNCs carrying different nascent chains of various lengths were prepared by translation of 3′-truncated mRNAs[4]. The RNCs are designated by the type of nascent chain—for instance, leader peptidase (Lep) or HemK—and the length of the nascent chain in numbers of amino acids—for example, Lep28-RNC.

To examine the kinetic stability of pre-formed SRP–ribosome complexes, we induced their dissociation by rapidly mixing complexes containing fluorescence-labeled SRP with excess unlabeled SRP (**Fig. 1a**). The stopped-flow traces revealed a dissociation pattern with up to three phases and apparent dissociation rates ranging from 150 s^{-1} to 0.01 s^{-1}. For an initial examination, we compared the approximate half-life times of complex dissociation, disregarding the multiphasic nature of the traces. The approximate half-life of the SRP complex with Lep50-RNCs (3 s) was much longer than that of the complex with non-translating ribosomes (10 ms), consistent with their respective equilibrium dissociation constants (K_d)[4]. The complex of SRP with HemK75-RNC exposing a non-SAS sequence dissociated slightly faster (**Fig. 1a**), in keeping with the lower affinity of that complex[4] (**Table 1**).

Previous equilibrium measurements have shown that RNCs with short nascent peptides (about 30–35 amino acids) of any sequence in which the nascent peptide is confined within the exit tunnel bind SRP with high affinity (K_d around 1 nM)[4]. The approximate half-life of the SRP complex with the Lep35-RNC was about 0.5 s (**Fig. 1a**), intermediate between those of the complexes with Lep50-RNCs and non-translating ribosomes. This difference suggests that (i) the binding of SRP to non-translating ribosomes, or to the HemK75-RNC exposing a non-SAS sequence, is transient; (ii) RNCs that carry a nascent peptide in the exit tunnel but do not yet expose the SAS retain SRP longer than non-translating ribosomes; and (iii) the exposure of an SAS leads to tight binding of SRP.

Kinetics of SRP–ribosome complex formation

To dissect the mechanism by which SRP discriminates between non-translating ribosomes and various RNCs, we analyzed the kinetics of SRP–ribosome complex formation at various concentrations of SRP (**Fig. 1b** and **Supplementary Fig. 1**). Fitting the stopped-flow traces required an expression with three exponential terms. In all cases, the rate of the first rapid step (k_{app1}) increased linearly with the SRP concentration, whereas the rates of the two slower steps (k_{app2} and k_{app3}) showed hyperbolic concentration dependencies (**Supplementary Fig. 2**). These results indicate a mechanism in which the binding step is followed by two sequential rearrangements (**Fig. 1c**). This suggests that after the initial binding of SRP to the ribosome, the complex undergoes dynamic fluctuations between three conformational states. The three states of the different complexes are probably related but are not structurally identical, as is evident from their differing kinetic behavior. Nevertheless, for simplicity, the three states and the corresponding rate constants are labeled the same for the different ribosome–SRP complexes. Elemental rate constants of the three steps were calculated by global fitting (**Supplementary Note**) of the data sets obtained by combining the time courses of binding at different SRP concentrations with the time courses of dissociation and with K_d values determined by equilibrium titration (**Table 1**). The results of the global fits are depicted in the figures along with the respective time courses, and rate constants are summarized in **Table 1**.

The forward rate constants of the three steps of ribosome–SRP complex formation, k_1 to k_3, are quite similar for all complexes studied, whereas the backward rate constants differ considerably. The finding that the k_1 values are similar suggests that the initial recruitment of SRP to the ribosome is independent of the presence of an SAS. The rate constants of the ensuing rearrangements indicate highly dynamic fluctuations of SRP between three states on any type of ribosome. The dissociation rate constant of the state 1 complex,

Table 1 Kinetic parameters of SRP–ribosome complex formation[a]

	Nt-R[b]	HemK75-RNC	Lep50-RNC	Lep35-RNC	Nt-R + Lep
k_1, μM^{-1} s^{-1}	175 ± 15	173 ± 10	150 ± 5	115 ± 5	100 ± 5
k_{-1}, s^{-1}	125 ± 5	118 ± 5	100 ± 2	14 ± 1	50 ± 2
k_2, s^{-1}	44 ± 3	21 ± 2	30 ± 1	30 ± 1	7 ± 1
k_{-2}, s^{-1}	8 ± 1	3.4 ± 0.3	2.4 ± 0.1	2.1 ± 0.3	1.2 ± 0.1
k_3, s^{-1}	0.8 ± 0.1	0.1 ± 0.05	1.4 ± 0.1	1.0 ± 0.1	0.4 ± 0.1
k_{-3}, s^{-1}	0.4 ± 0.1	0.27 ± 0.05	0.010 ± 0.005	0.35 ± 0.05	0.05 ± 0.01
k_{off}, s^{-1}[c]	10	15	0.08	1.0	1.0
K_d, nM[d]	60 ± 5	350 ± 30	2 ± 1	3.5 ± 0.5	10 ± 2

[a]Rate constants were estimated by global fitting of time courses of dissociation (**Fig. 1a**) and binding (**Supplementary Fig. 2**), using a three-step kinetic model (**Fig. 1c** and **Supplementary Note**). [b]Nt-R, non-translating ribosomes. [c]Average dissociation rate constants, as calculated from backward rate constants and the relative population of states 1, 2, and 3 of the SRP–ribosome complexes (**Fig. 1c**). [d]K_d values determined by titration (**Supplementary Fig. 3**). K_d values calculated from the rate constants match those determined by titration within a factor of 2–3.

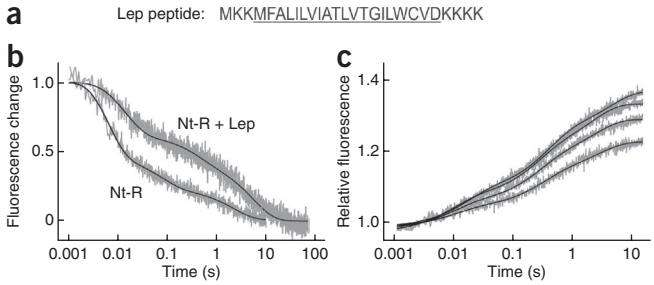

Figure 2 Influence of the Lep peptide on the kinetics of SRP–ribosome interaction. (**a**) Amino acid sequence of the Lep peptide. The SAS is underlined. (**b**) SRP–ribosome complex dissociation. Complexes of MDCC-labeled non-translating ribosomes and Bpy-labeled SRP were formed either in the absence or presence of the Lep peptide (5 μM). Dissociation was induced by rapidly mixing the complex with unlabeled SRP as in **Figure 1a**. (**c**) SRP complex formation with non-translating ribosomes. Time courses were measured in the presence of the Lep peptide (5 μM) at increasing concentrations of SRP (bottom to top: 0.1, 0.15, 0.2, 0.3 μM) as in **Supplementary Figure 2**. Global fitting was performed as for the data of **Figure 1**, and the results are shown as smooth lines.

k_{-1}, is similar for non-translating ribosomes and Lep50-RNCs. Thus, the higher affinity of SRP binding to Lep50-RNCs in comparison with non-translating ribosomes is mainly due to the much lower backward rate constant k_{-3}, whereas the other rate constants are comparable (values of k_{-2} differ only within a factor of about 3). For the Lep35-RNC–SRP complex, the results of the kinetic analysis reveal differences in the values of k_{-1} and k_{-3} that partly counterbalance each other, consistent with our previous observation of similar affinities of SRP binding to Lep35- and Lep50-RNCs. In comparison, the SRP complex with HemK75-RNC rearranges to state 3 ten times more slowly. This is in line with the low affinity of that complex and indicates that a non-SAS sequence exposed on the ribosome sterically interferes with SRP binding.

From the rate constants, we estimated the internal equilibria between the three fluctuating conformational states for the different complexes. The complex with Lep50-RNC is almost completely (97%) locked in state 3, which is particularly stable when compared to the corresponding states of the other complexes. As a result, SRP is released from that complex very slowly, with an average rate constant of $k_{off} = 0.08\ s^{-1}$, as calculated from the three backwards rate constants and the population of states 1, 2, and 3 of the complex (**Table 1**). Note that the average dissociation rate constant is independent of fluorescence changes and represents an effective rate at which SRP dissociates from the ribosome.

The distribution of SRP between the three conformational states on non-translating ribosomes was state 1:state 2:state 3 = 6:31:63%, and the back reactions from any of these states were rapid, resulting in a high average dissociation rate constant, $k_{off} = 10\ s^{-1}$. For the complex with HemK75-RNC the average k_{off} was even higher, about $15\ s^{-1}$. A similar distribution between the three states was found with Lep35-RNC, 2:25:73%. For the latter complex, the value of k_{-3} remained relatively high, indicating a low stability of state 3; however, due to lower values of k_{-1} and k_{-2}, the average k_{off} of SRP dissociation from Lep35-RNC was decreased to $1\ s^{-1}$.

Influence of the Lep peptide on SRP–ribosome complexes

The results obtained with Lep50-RNCs demonstrated the strong influence of the binding of the exposed SAS and SRP on the kinetic stability of the ribosome–SRP complex, in particular the stability of the locked state 3 of the complex. To study the effects of SRP binding to the ribosome and to the SAS separately, we performed experiments in which we added an oligopeptide of 28 amino acids encompassing the SAS of leader peptidase, referred to as Lep peptide (**Fig. 2a**). The Lep peptide bound to SRP with a K_d of 0.8 ± 0.2 μM, as determined by equilibrium titration (**Supplementary Fig. 3**), which is comparable to the affinities reported for the binding of the isolated LamB or EspP signal peptides to *E. coli* SRP[10,11].

In the presence of the Lep peptide, the affinity of SRP binding to non-translating ribosomes was increased (**Supplementary Fig. 3**). The stabilization was due to the slower dissociation of the SRP complex with non-translating ribosomes (**Fig. 2b**) as well as to altered kinetics of complex formation (**Fig. 2c** and **Table 1**). The main kinetic effect of Lep peptide binding to SRP was the stabilization of state 3 of the SRP complex with non-translating ribosomes (k_{-3} lower by a factor of 10); in addition, the rate constants k_2 and k_{-2} were lowered. The distribution between states 1, 2 and 3 was 2:11:87%, intermediate between the values found for the SRP complexes with non-translating ribosomes and Lep50-RNCs, and the average k_{off} of the complex was $1.1\ s^{-1}$. Thus, the Lep peptide brought the complex into a state that kinetically resembled the complex with Lep35-RNC, but it was not sufficient to bring the SRP into the fully locked state observed with Lep50-RNC.

The stabilizing effect of the Lep peptide was comparable with Lep28-RNC containing a nascent peptide within the exit tunnel or with HemK75-RNC with an exposed non-SAS peptide (**Fig. 3**). With Lep35-RNC the stabilizing effect of the Lep peptide was smaller, possibly because in Lep35-RNC part of the nascent peptide may already emerge from the exit tunnel and may, by binding to SRP, impair binding of the Lep peptide. In the case of Lep50-RNC, where the SAS-binding site of SRP is occupied by the Lep SAS exposed on the ribosome, the addition of the Lep peptide had no stabilizing effect.

Interaction of FtsY with SRP and SRP–ribosome complexes

We studied the kinetics of FtsY–SRP complex formation and dissociation by measuring FRET between SRP (labeled with the donor Alexa555 at position 152 of Ffh) and FtsY (labeled with the non-fluorescent acceptor QSY9 at position 342) by monitoring the

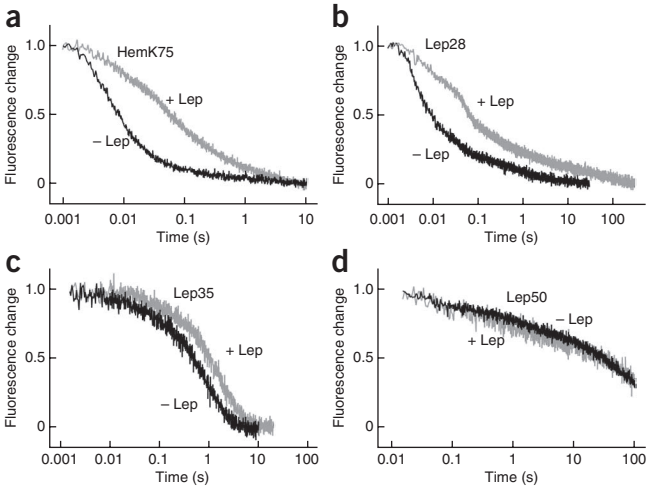

Figure 3 Influence of the Lep peptide on the kinetic stability of SRP–RNC complexes. (**a**–**d**) Shown are dissociation kinetics for HemK75-RNC (**a**), Lep28-RNC (**b**), Lep35-RNC (**c**) and Lep50-RNC (**d**). Complexes of MDCC-labeled RNCs and Bpy-labeled SRP were formed in the absence or presence of Lep peptide (5 μM). Dissociation was induced by rapidly mixing the complexes with unlabeled SRP as in **Figure 1a**.

Table 2 Kinetic parameters of FtsY–SRP complex formation[a]

Parameter	SRP	SRP–nt-R[b]	SRP–Lep50-RNC	SRP–Lep35-RNC	SRP–Lep–nt-R
k_1, $\mu M^{-1}\ s^{-1}$	5 ± 1	8 ± 1	8 ± 1	9 ± 2	9 ± 1
k_{-1}, s^{-1}	8 ± 2	1.6 ± 0.3	1.6 ± 0.3	1.5 ± 0.3	1.4 ± 0.2
k_2, s^{-1}	0.14 ± 0.05	0.12 ± 0.05	0.7 ± 0.2	0.7 ± 0.2	0.9 ± 0.2
k_{-2}, s^{-1}	0.05 ± 0.02	0.05 ± 0.02	0.07 ± 0.02	0.1 ± 0.03	0.2 ± 0.05
K_d, nM[c]	700 ± 100	250 ± 50	5 ± 1	7 ± 2	20 ± 5

[a]Rate constants were estimated by global fitting of time courses of dissociation (**Fig. 4a**) and binding (**Fig. 4b**), using a two-step kinetic model (**Fig. 4c**; see Online Methods). [b]Nt-R, non-translating ribosomes. [c]K_d values determined by titration (**Supplementary Fig. 4**). K_d values calculated from the rate constants match the values determined by titration within a factor of 3–4.

fluorescence of the donor; the signal from a single fluorescent label, Bpy, at position 342 in FtsY provided additional information. GTP, which is required for stable complex formation between SRP and FtsY, was replaced with the non-hydrolyzable analog GDPNP to avoid GTP hydrolysis.

Previous equilibrium measurements revealed that the affinity of FtsY binding to SRP (K_d = 0.1–0.3 μM)[12–15] remained essentially unchanged when SRP was bound to non-translating ribosomes (≈0.3 μM) but increased (K_d = 5 nM) when SRP was bound to Lep50-RNCs[4]. The labeled components used for kinetic analysis yielded comparable K_d values (**Supplementary Fig. 4** and **Table 2**). Competition experiments showed that the dissociation kinetics are not different for the different ribosome–SRP–FtsY complexes (**Fig. 4a**)—that is, the ribosome-induced gain in SRP-FtsY affinity was not due to lowering k_{off}, suggesting it reflects an increase of k_{on}.

FtsY binding to SRP or various SRP–ribosome complexes gave rise to a decrease of donor fluorescence that could be described by two main exponential terms, indicating a two-step mechanism of complex formation (**Fig. 4b**). The concentration dependence of the rate of the first step (k_{app1}) was linear in all cases studied (**Supplementary Fig. 5**), indicating a second-order binding step. The slower step (k_{app2}) showed a hyperbolic concentration dependence, indicating that it represents a rearrangement after the formation of the initial binding complex (**Fig. 4c**). Global fitting of the time courses measured at different concentrations of FtsY together with the dissociation time courses (**Supplementary Note**) yielded the rate constants for SRP–FtsY complex formation and dissociation (**Table 2**). The values of k_1 and k_{-1} were similar for all complexes. The values of k_{-2} were between 0.05 s^{-1} and 0.2 s^{-1} for the ribosome complexes, as well as for the complex of FtsY with unbound SRP. By contrast, k_2 was about six times higher for FtsY binding to SRP bound to Lep35- or Lep50-RNC than for FtsY binding to SRP bound to non-translating ribosomes or unbound SRP. This indicates that the affinity increase of FtsY binding to SRP, which is a consequence of high-affinity binding of SRP to RNCs, is predominantly due to an acceleration of the rearrangement step, as reflected in the increase of the forward rate constant k_2. The SRP–FtsY complex formed in the absence of ribosomes was rather unstable, reflected in a high value of k_{-1} (8 s^{-1}) compared to about 1.5 s^{-1} for the ribosome-bound complex.

The Lep peptide added in *trans* increased k_2 of FtsY binding to SRP on non-translating ribosomes by nearly a factor of 10 (**Table 2**). Thus, binding of the isolated Lep peptide to SRP influences the interaction of FtsY with SRP on the ribosome in a similar way as the exposed nascent SAS on Lep50-RNC does. On RNC–SRP complexes with filled exit tunnel, as in Lep28-RNC, binding of the Lep peptide lowered the K_d only slightly (**Supplementary Fig. 5**), probably because the presence of the nascent chain already enhances the affinity of FtsY binding more than ten times, leaving less room for further enhancement. The small stabilizing effect is probably due to an increased rate of complex formation (increased k_2), as with non-translating ribosomes (**Table 2**), although the effect was too small to be determined with precision.

DISCUSSION

The present kinetic analysis reveals that SRP can rapidly scan ribosomes in all functional states, including non-translating ones or RNCs exposing non-SAS sequences, until it encounters a translating ribosome with either the exit tunnel just filled or one exposing a signal sequence (**Fig. 5**). When the nascent peptide has reached a length of about 30 amino acids, the complex is switched from the scanning to the standby mode, from which SRP is released ten times less rapidly than from non-translating ribosomes. The standby position enables SRP to bind an SAS as soon as it emerges from the exit tunnel. Upon recognition of an SAS, SRP is stabilized in a state in which it dissociates approximately 100 times slower than from non-translating ribosomes (0.08 s^{-1} versus 10 s^{-1}). This affinity switch turns SRP into the targeting mode and leads to the accelerated recruitment of the SRP receptor to form a stable targeting complex. In contrast, if a non-cognate sequence emerges, SRP loses its affinity for the RNC and is released rapidly (15 s^{-1}) to resume scanning, and the non-cognate RNC is rejected from targeting.

In our system, the initial binding of SRP to the ribosomes is very rapid, ≈10^8 M^{-1} s^{-1}, and largely independent of the presence of an SAS on the ribosome (**Table 1**). Notably, the ribosomes used in this work are fully active in translation and the nascent Lep peptide in the RNCs has its native sequence. A value lower by a factor of 50 for the

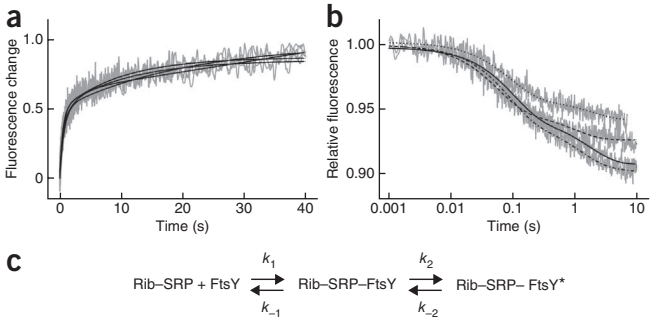

Figure 4 Kinetics of FtsY interaction with ribosome-bound SRP. (**a**) Dissociation of FtsY from SRP. The complexes of SRP(Alx152) (0.1 μM) and FtsY(QSY342) (1 μM) with non-translating ribosomes (0.5 μM), non-translating ribosomes with Lep peptide (5 μM), Lep35-RNCs (0.085 μM) or Lep50-RNCs (0.085 μM) were rapidly mixed with unlabeled FtsY (5 μM). Complex dissociation was monitored by the increase of donor (Alx) fluorescence due to the release of the FRET acceptor. Elemental rate constants were obtained by global fitting (**Supplementary Note** and **Table 2**); the functions calculated with these constants are shown as smooth lines. Dissociation rates were the same for the three complexes in the absence and presence of the Lep peptide. (**b**) FtsY binding to SRP. SRP(Alx152) (0.1 μM) was bound to non-translating ribosomes (0.5 μM; continuous fitted line), non-translating ribosomes in the presence of Lep peptide (5 μM; dashed-dotted line), Lep35-RNCs (0.085 μM; dotted line) or Lep50-RNCs (0.085 μM; dashed line), and the complexes were rapidly mixed with FtsY(QSY342) at concentrations up to 4 μM; traces shown were obtained at 1 μM. The decrease of donor (Alx) fluorescence due to FRET was monitored. Rate constants (**Table 2**) were determined by global fitting (**Supplementary Note**). The functions calculated with the rate constants are shown as fitted lines. (**c**) Two-step scheme of FtsY–SRP complex formation. Rib, ribosome.

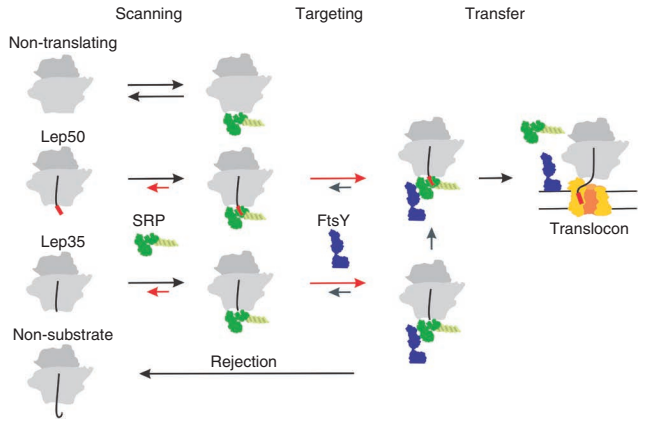

Figure 5 Schematic of the SRP cycle derived from kinetics. The model depicts the kinetically controlled switch from the scanning to the targeting mode of SRP and the decision made between RNC transfer to the translocon and rejection, on the basis of the appearance of an SAS (depicted in red) or non-signal sequence, respectively, outside the ribosome. Depending on the functional state of the ribosome (non-translating or translating) and the nature of the RNC (short or long nascent peptide; absence or presence of SAS), forward and backward reactions are kinetically favored (large red arrows) or disfavored (small red arrows). GTP binding to SRP and FtsY and GTP hydrolysis during RNC transfer to the translocon are not shown.

association rate constant, k_{on}, was reported by Shan and colleagues[16], who used SecM-stalled RNCs with nascent FtsQ carrying a triple strep tag at the N terminus[14] and a fluorophore incorporated into an internal position of the nascent peptide. The low on-rate indicates that these complexes are compromised in the kinetics of SRP binding. One possibility may be that the SecM stalling sequence, which blocks the peptidyl transferase center allosterically via interactions in the exit tunnel[15], also influences SRP binding at the tunnel exit.

When bound to the ribosome, SRP undergoes dynamic fluctuations, manifested as reversible rearrangements between states 1, 2 and 3. We note that the three states identified by kinetic analysis may not be the only discrete states of SRP on the ribosome. Rather, SRP may sample a continuum of states, some of which are populated enough to be distinguished by their FRET signals. We show that the initial recruitment of SRP to the ribosome is followed by rapid and reversible rearrangements that can be interpreted as SRP probing the conformational landscape of the ribosome in search for additional interactions. Non-translating ribosomes, or ribosomes exposing a non-SAS sequence, do not provide these contacts, allowing SRP to dissociate rapidly and to sample (or re-sample) many ribosomes until it encounters a ribosome with the exit tunnel filled or exposing an SAS. The presence of a nascent peptide in the tunnel changes the interactions at the SRP docking site, presumably by signaling through protein L23 (ref. 4), and alters the fluctuation dynamics of SRP, thereby slowing down the release of SRP from the ribosome. An emerging SAS (or an SAS-containing peptide added in *trans*) additionally stabilizes SRP binding. The two effects appear to be additive, each decreasing the average dissociation rate of the SRP-ribosome complex about ten times (**Table 1**), resulting in an overall stabilization of SRP binding by two orders of magnitude.

The targeting complex is formed when ribosome-bound SRP binds to the SRP receptor, FtsY. The interaction, which is relatively weak on non-translating ribosomes, is strengthened considerably on RNCs exposing an SAS[4]. The SAS binds into a groove in the M domain of Ffh that is lined with hydrophobic amino acids. According to the crystal structure of the SRP54 protein (the eukaryotic or archaeal homolog to Ffh) fused to a signal peptide, binding of the signal peptide induces a large conformational change toward an open structure of SRP54 in which the G domain has moved away from the M domain[17]. An open conformation was also observed for a similar signal peptide–SRP54 fusion bound to SRP RNA[18]. The electron-microscopic reconstruction of the SRP complex with RNCs exposing a signal peptide revealed the same conformation of SRP[9]. The present kinetic analysis reveals that the affinity increase is predominantly due to the acceleration of a rearrangement of the initial binding complex (**Table 2**). The acceleration is observed for the SRP complexes with translating ribosomes, either Lep35-RNC or Lep50-RNC, or non-translating ribosomes in the presence of the Lep peptide. Apparently, in all these complexes SRP is present in a conformation that is poised for the interaction with FtsY, in line with the open conformation of SRP on the ribosome[8,9] and the structure of the heterodimeric complex of the NG domains[19,20]. A similar arrangement is seen in the electron-microscopic reconstruction of an 'early' RNC–SRP–FtsY complex formed without GTP[21]. In the cell, the formation of the targeting complex may also be affected by the interactions of FtsY with the translocon and membrane lipids[22,23], as lipids influence FtsY–SRP complex formation by inducing a conformational change of the A domain of FtsY[24].

The initial association of FtsY with unbound SRP is rapid, $k_1 = 5\ \mu M^{-1}\ s^{-1}$, and is accelerated very little when SRP is bound to the ribosome or Lep-RNCs (**Table 2**). The kinetic parameters of the present initial complex are similar to those of the 'early' complex, formed between FtsY and SRP bound to RNCs exposing the SAS of FtsQ[25]. However, the 'closed' complex in that work apparently is much less stable (backward rate constant $\approx 1\ s^{-1}$) than the present targeting complex, Lep50-RNC–SRP–FtsY*, which rearranges back with a rate constant of $k_{-2} = 0.07\ s^{-1}$. This kinetic difference is reflected in different K_d values of the respective complexes, 40 nM (ref. 25) and 5 nM[4]. Another large difference we note involves the affinity of FtsY for SRP bound to non-translating ribosomes, 5.2 μM (ref. 26), as compared to submicromolar K_d values from the present analysis (**Table 2**) or previous equilibrium titrations[4,8]. The discrepancies may be caused by differences in the preparations used for the experiments. However, there are also differences in the kinetic analyses. We have determined elemental rate constants by global fitting of the combined time courses of complex dissociation and formation, the latter measured over a wide range of concentrations. By contrast, the earlier analyses[25,27] used linear approximations based on data points obtained at rather low concentrations (up to 0.25 μM) far from saturation. The values for k_{on} and k_{off} obtained that way do not represent elemental steps and cannot be compared with the rate constants we have determined. We also note that a stable targeting complex, like the one we observe, is more consistent with current models of targeting RNCs to the translocon, in which the SRP-FtsY interaction is resolved only upon GTP hydrolysis that takes place concomitantly with, or after, RNC transfer to the translocon.

In conclusion, the present analysis reveals that the targeting complex, consisting of ribosomes, SRP, and FtsY, is strongly stabilized when SRP recognizes an SAS on translating ribosomes. A similar, somewhat smaller effect is brought about by an SAS-containing peptide added in *trans*. The stabilization of the interaction of SRP with the ribosome is mainly due to a decreased dissociation rate constant of state 3 of the complex, k_{-3} (**Fig. 1c**). This suggests that the rearrangement of state 2 to state 3 of the RNC–SRP complex is promoted by SAS binding to SRP. FtsY presumably binds predominantly to state 3, as the rates of both forward reactions of targeting complex formation are accelerated when SRP is bound to Lep50-RNC. The resulting complex

is rather stable, suggesting that GTP hydrolysis by both SRP and FtsY is required to disrupt the complex. Our kinetic analysis shows how dynamic fluctuations of the SRP–RNC complexes govern the selection of RNCs exposing an SAS for targeting to the translocon.

METHODS

Methods and any associated references are available in the online version of the paper.

Note: Supplementary information is available in the online version of the paper.

ACKNOWLEDGMENTS

We thank E. Deuerling (University of Konstanz, Germany) for the *E. coli* strain lacking ribosomal protein L23 and A. Bursy, F. Hummel, T. Wiles, S. Kappler and O. Geintzer for expert technical assistance. The work was supported by the Deutsche Forschungsgemeinschaft (grant WI 626/18-1 to W.W.).

AUTHOR CONTRIBUTIONS

W.H., T.B., M.V.R. and W.W. conceived the research and designed experiments. W.H. and S.L. prepared materials and conducted experiments. W.H., S.L., T.S. and M.V.R. analyzed the data. W.W. and M.V.R wrote the paper.

COMPETING FINANCIAL INTERESTS

The authors declare no competing financial interests.

Published online at http://www.nature.com/doifinder/10.1038/nsmb.2421.
Reprints and permissions information is available online at http://www.nature.com/reprints/index.html.

1. Bibi, E. Early targeting events during membrane protein biogenesis in *Escherichia coli*. *Biochim. Biophys. Acta* **1808**, 841–850 (2011).
2. Grudnik, P., Bange, G. & Sinning, I. Protein targeting by the signal recognition particle. *Biol. Chem.* **390**, 775–782 (2009).
3. Luirink, J., von Heijne, G., Houben, E. & de Gier, J.W. Biogenesis of inner membrane proteins in *Escherichia coli*. *Annu. Rev. Microbiol.* **59**, 329–355 (2005).
4. Bornemann, T., Jöckel, J., Rodnina, M.V. & Wintermeyer, W. Signal sequence-independent membrane targeting of ribosomes containing short nascent peptides within the exit tunnel. *Nat. Struct. Mol. Biol.* **15**, 494–499 (2008).
5. Zhang, X., Rashid, R., Wang, K. & Shan, S.O. Sequential checkpoints govern substrate selection during cotranslational protein targeting. *Science* **328**, 757–760 (2010).
6. Jensen, C.G. & Pedersen, S. Concentrations of 4.5S RNA and Ffh protein in *Escherichia coli*: the stability of Ffh protein is dependent on the concentration of 4.5S RNA. *J. Bacteriol.* **176**, 7148–7154 (1994).
7. Gu, S.Q., Peske, F., Wieden, H.J., Rodnina, M.V. & Wintermeyer, W. The signal recognition particle binds to protein L23 at the peptide exit of the *Escherichia coli* ribosome. *RNA* **9**, 566–573 (2003).
8. Buskiewicz, I.A., Jockel, J., Rodnina, M.V. & Wintermeyer, W. Conformation of the signal recognition particle in ribosomal targeting complexes. *RNA* **15**, 44–54 (2009).
9. Halic, M. *et al.* Signal recognition particle receptor exposes the ribosomal translocon binding site. *Science* **312**, 745–747 (2006).
10. Zheng, N. & Gierasch, L.M. Domain interactions in *E. coli* SRP: stabilization of M domain by RNA is required for effective signal sequence modulation of NG domain. *Mol. Cell* **1**, 79–87 (1997).
11. Bradshaw, N., Neher, S.B., Booth, D.S. & Walter, P. Signal sequences activate the catalytic switch of SRP RNA. *Science* **323**, 127–130 (2009).
12. Jagath, J.R., Rodnina, M.V., Lentzen, G. & Wintermeyer, W. Interaction of guanine nucleotides with the signal recognition particle from *Escherichia coli*. *Biochemistry* **37**, 15408–15413 (1998).
13. Peluso, P. *et al.* Role of 4.5S RNA in assembly of the bacterial signal recognition particle with its receptor. *Science* **288**, 1640–1643 (2000).
14. Schaffitzel, C. & Ban, N. Generation of ribosome nascent chain complexes for structural and functional studies. *J. Struct. Biol.* **158**, 463–471 (2007).
15. Bhushan, S. *et al.* SecM-stalled ribosomes adopt an altered geometry at the peptidyl transferase center. *PLoS Biol.* **9**, e1000581 (2011).
16. Saraogi, I., Zhang, D., Chandrasekaran, S. & Shan, S.O. Site-specific fluorescent labeling of nascent proteins on the translating ribosome. *J. Am. Chem. Soc.* **133**, 14936–14939 (2011).
17. Janda, C.Y. *et al.* Recognition of a signal peptide by the signal recognition particle. *Nature* **465**, 507–510 (2010).
18. Hainzl, T., Huang, S., Merilainen, G., Brannstrom, K. & Sauer-Eriksson, A.E. Structural basis of signal-sequence recognition by the signal recognition particle. *Nat. Struct. Mol. Biol.* **18**, 389–391 (2011).
19. Egea, P.F. *et al.* Substrate twinning activates the signal recognition particle and its receptor. *Nature* **427**, 215–221 (2004).
20. Focia, P.J., Shepotinovskaya, I.V., Seidler, J.A. & Freymann, D.M. Heterodimeric GTPase core of the SRP targeting complex. *Science* **303**, 373–377 (2004).
21. Estrozi, L.F., Boehringer, D., Shan, S.O., Ban, N. & Schaffitzel, C. Cryo-EM structure of the *E. coli* translating ribosome in complex with SRP and its receptor. *Nat. Struct. Mol. Biol.* **18**, 88–90 (2011).
22. Mircheva, M. *et al.* Predominant membrane localization is an essential feature of the bacterial signal recognition particle receptor. *BMC Biol.* **7**, 76 (2009).
23. Braig, D. *et al.* Signal sequence-independent SRP-SR complex formation at the membrane suggests an alternative targeting pathway within the SRP cycle. *Mol. Biol. Cell* **22**, 2309–2323 (2011).
24. Stjepanovic, G. *et al.* Lipids trigger a conformational switch that regulates signal recognition particle (SRP)-mediated protein targeting. *J. Biol. Chem.* **286**, 23489–23497 (2011).
25. Zhang, X., Schaffitzel, C., Ban, N. & Shan, S.O. Multiple conformational switches in a GTPase complex control co-translational protein targeting. *Proc. Natl. Acad. Sci. USA* **106**, 1754–1759 (2009).
26. Shen, K., Zhang, X. & Shan, S.O. Synergistic actions between the SRP RNA and translating ribosome allow efficient delivery of the correct cargos during cotranslational protein targeting. *RNA* **17**, 892–902 (2011).
27. Zhang, X., Kung, S. & Shan, S.O. Demonstration of a multistep mechanism for assembly of the SRP x SRP receptor complex: implications for the catalytic role of SRP RNA. *J. Mol. Biol.* **381**, 581–593 (2008).

ONLINE METHODS

Preparations and fluorescence labeling. 4.5S RNA and mRNAs coding for the first 35 or 50 amino acids of leader peptidase were prepared by *in vitro* transcription of linearized DNA generated from the plasmids pT7-4.5S for 4.5S RNA and pBSK2-LepB for different lengths of Lep mRNAs, respectively, using Phusion polymerase (Biozym Scientific). Proteins Ffh and FtsY, both extended by six histidines at the C terminus, were expressed from plasmids pET24-Ffh and pET9-FtsY, respectively, using the *E. coli* strain BL21(DE3)pLysS, and purified as previously described[28]. Base exchanges for the cysteine substitution of amino acids at positions 152, 181, and 430 of Ffh and position 342 of FtsY were performed by QuikChange PCR mutagenesis using Phusion polymerase. Mutations were confirmed by DNA sequencing. Mutant proteins were expressed and purified as the wild-type proteins were. The Lep peptide was purchased from Panatecs GmbH (Tübingen, Germany).

Labeling of cysteine-substituted Ffh and FtsY with the maleimide derivatives of the respective dyes was carried out by incubation with a ten-fold excess of dye over protein in buffer A (25 mM HEPES, pH 7.5; 70 mM NH_4Cl; 30 mM Kcl; 7 mM $MgCl_2$) for 1 hr at 25 °C. Maleimide derivatives of Alexa Fluor555 (Alx), Bodipy-FL (Bpy), MDCC, and QSY9 (QSY) were from Life Technologies Corporation. Unreacted dye was removed by chromatography on HiTrapQ HP (FtsY) or HiTrap SP HP (Ffh) columns. The extent of labeling was about 90%, as determined by absorption measurements and SDS-PAGE. Cysteine substitution and dye insertion did not affect the activity of Ffh in binding to 4.5S RNA or the binding of SRP containing labeled Ffh to FtsY or to ribosomes[29]. Labeled FtsY was fully active in binding to SRP.

SRP was prepared by mixing Bpy-labeled or unlabeled Ffh with 4.5S RNA (1.2-fold molar excess) in buffer A and incubating for 10 min at 25 °C.

Fluorescence labeling of protein L23 in 50S ribosomal subunits. To introduce a fluorescent label at the binding site of SRP on the 50S ribosomal subunit, we replaced Ser21 in protein L23 with cysteine. For the expression of ribosomes carrying mutant L23, we used the *E. coli* strain MC4100, in which the chromosomal gene for L23 had been deleted[30]. The plasmid pTrc99B coding for wild-type L23 contained in strain MC4100 was exchanged for the plasmid coding for mutant L23, derived from the pCDF duet vector. Ribosomes containing mutant L23 were isolated in the same way as wild-type ribosomes[31]. Ribosomal subunits were prepared by zonal centrifugation[32].

For fluorescence labeling, 50S subunits containing mutant protein L23 (6 nmol) were incubated in 0.4 ml of buffer A with MDCC maleimide (1.1 µmol; ten-fold excess over the 19 cysteine residues present in mutant 50S subunits) for 1 h at 25 °C. The reaction was terminated by the addition of 2-mercaptoethanol (10 mM). To remove unreacted dye, the 50S subunits were centrifuged through a sucrose cushion (1.1 M, 400 µl) in buffer A with 20 mM Mg^{2+} for 2 h at 259,000*g*. The pellet was dissolved in buffer A (7 mM Mg^{2+}) and stored at −80 °C. The extent of labeling of protein L23 was about 85%, as determined by SDS-PAGE and western blot analysis. Unspecific labeling at intrinsic cysteine residues, as determined with wild-type 50S subunits, amounted to an average of about four molecules of MDCC per 50S subunit, as determined photometrically. Upon binding labeled SRP, 70S ribosomes prepared from those 50S subunits showed residual fluorescence changes (≈20% of the signal observed with the label on L23).

To obtain functional 70S ribosomes, labeled 50S subunits were associated with an equimolar amount of unmodified 30S subunits in buffer A for 30 min at 37 °C; the 30S subunits had been activated by incubation in buffer A with 20 mM Mg^{2+} for 30 min at 37 °C. The re-associated MDCC-labeled ribosomes were as active as the wild-type control in initiation complex formation (>90%), dipeptide formation (>85%) and translation of Lep mRNA (>80%).

RNC preparation. Ribosomes from *E. coli* MRE600, initiation factors IF1, IF2, and IF3, EF-Tu, EF-G, f[^{3}H]Met-tRNA^{fMet} and total tRNA were prepared as described[31]. RNCs were prepared by *in vitro* translation of mRNAs with truncated coding sequence, as described previously[4], using MDCC-labeled ribosomes where indicated. In the RNC preparations used for the present experiments, about 80% of the ribosomes carried the respective peptide chain, except when indicated otherwise.

Rapid kinetics. The kinetics of the interaction of SRP, FtsY and ribosomes were analyzed by stopped flow (SX-20MV; Applied Photophysics). SRP binding to ribosomes was measured in buffer C (25 mM HEPES, pH 7.5; 70 mM ammonium acetate; 30 mM potassium acetate; 7 mM magnesium acetate; 10% glycerol) in the presence of 0.5 mM GDPNP at 25 °C. Association kinetics of SRP binding to ribosomes were measured by monitoring the change of FRET after rapidly mixing equal volumes (55 µl) of the solution of MDCC-labeled ribosomes or RNCs (0.025 µM final concentration after mixing) with solutions of increasing concentrations of Bpy-labeled SRP (acceptor). The FRET donor MDCC was excited at 410 nm, and the emission of the FRET acceptor Bpy was measured after passing a cut-off filter (KV530; Schott). The dissociation of SRP from ribosomes and RNCs was induced by chase with excess non-labeled SRP. Complexes for chase were prepared by incubating fluorescence-labeled non-translating ribosomes (0.1 µM) or RNCs (0.2 µM) with labeled SRP (1 µM and 0.2 µM, respectively) for 2 min. To induce dissociation, the complexes were rapidly mixed with a ten-fold excess of unlabeled SRP, and the decrease of acceptor fluorescence was monitored.

FtsY binding to SRP or SRP–ribosome complexes was measured in buffer C, which additionally contained 0.015% Nikkol, in the presence of 0.5 mM GDPNP at 25 °C. Nikkol was added to facilitate handling FtsY at the high concentrations required for the kinetic experiments. Control experiments showed that the detergent had no influence on the binding of FtsY to SRP or SRP to ribosomes in either in the absence or the presence of the Lep peptide (data not shown). The kinetics of the interaction of FtsY with SRP or ribosome-bound SRP was examined by stopped flow, monitoring FRET between SRP (Alx555 at position 152 of Ffh) and FtsY (QSY9 at position 342). Alx555 fluorescence was excited at 520 nm, and the emission was measured after passing a cut-off filter (KV550, Schott). Association experiments were performed by rapidly mixing labeled FtsY (0.2–2 µM) with either labeled SRP alone (0.1 µM), SRP–ribosome complexes (0.1 µM SRP, 0.5 µM non-translating ribosomes), or SRP–RNC complexes (0.1 µM SRP, 0.085 µM RNC). In addition, the rearrangement of the FtsY complexes with SRP alone or various SRP–ribosome complexes was measured by stopped-flow, monitoring fluorescence changes of either FtsY(Bpy342) or SRP(MDCC181) directly, without FRET (data not shown). The results were similar to those for the second step as indicated by FRET.

The dissociation of labeled FtsY from labeled SRP–ribosome complexes was initiated by mixing with excess non-labeled FtsY and was monitored by FRET. Fluorescent labels were the same as those used above. SRP–ribosome–FtsY complexes (0.1 µM SRP, 0.5 µM non-translating ribosomes, 1 µM FtsY) or SRP–RNC–FtsY complexes (0.1 µM SRP, 0.085 µM RNC, 1 µM FtsY) were rapidly mixed with non-labeled FtsY (5 µM).

To obtain elemental rate constants, the kinetic data were evaluated both analytically and by global fit, as described in the **Supplementary Note**.

28. Buskiewicz, I., Kubarenko, A., Peske, F., Rodnina, M.V. & Wintermeyer, W. Domain rearrangement of SRP protein Ffh upon binding 4.5S RNA and the SRP receptor FtsY. *RNA* **11**, 947–957 (2005).
29. Buskiewicz, I. *et al.* Conformations of the signal recognition particle protein Ffh from *Escherichia coli* as determined by FRET. *J. Mol. Biol.* **351**, 417–430 (2005).
30. Kramer, G. *et al.* L23 protein functions as a chaperone docking site on the ribosome. *Nature* **419**, 171–174 (2002).
31. Rodnina, M.V. & Wintermeyer, W. GTP consumption of elongation factor Tu during translation of heteropolymeric mRNAs. *Proc. Natl. Acad. Sci. USA* **92**, 1945–1949 (1995).
32. Milon, P. *et al.* Transient kinetics, fluorescence, and FRET in studies of initiation of translation in bacteria. *Methods Enzymol.* **430**, 1–30 (2007).

doi:10.1038/nsmb.2421